

¹⁴N. Stump and G. Maier, Phys. Lett. 24A, 625 (1967).

¹⁵J. Kocinski and B. Mrygon, Phys. Lett. 28A, 386 (1968).

¹⁶D. Bally, B. Grabcev, A. M. Lungu, M. Popovici,

and M. Totia, J. Phys. Chem. Solids 28, 1947 (1967).

¹⁷S. Spooner and B. L. Averbach, Phys. Rev. 142, 291 (1966).

¹⁸L. Passell, private communication (see Ref. 4).

ORDER PARAMETER AND PHASE TRANSITIONS OF STRESSED SrTiO₃

K. A. Müller, W. Berlinger, and J. C. Slonczewski*

IBM Zurich Research Laboratory, 8803 Rüschlikon, Switzerland

(Received 6 July 1970)

EPR spectra of Fe-V_O pairs were used to study how the order parameter of SrTiO₃ varies with uniaxial stress applied to a (111) face. A second-order cubic-trigonal phase boundary appears above the stress-free transition temperature T_a . A first-order tetragonal-trigonal phase boundary is found below T_a . An independently determined Landau potential describes the results.

In this Letter we report effects of applied uniaxial stress on the structure of strontium titanate (SrTiO₃), a solid with a structural transition in the free state. We observe the variation of the order parameter with stress and temperature, construct phase boundaries from its behavior, and account for our results with the Landau theory.

Recent investigations have revealed the close connection between the cubic-to-trigonal and cubic-to-tetragonal transitions in LaAlO₃ and SrTiO₃, respectively, which occur in the absence of applied stress.¹⁻³ In each case the transition, with critical temperature T_a , results from an instability of an optic-mode displacement representing a rotation $\pm\bar{\varphi}$ of nearly rigid TiO₆^{4,5} or AlO₆^{6,7} octahedra.² Whether the trigonal ($R\bar{3}c$) or the tetragonal ($I4/mcm$) structure is realized depends on the ratio of fourth-order parameters in the Landau theory,³ if these parameters are adjusted for interaction with strain.⁸ In the lattice-Hamiltonian theory of Pytte and Feder⁹ this issue is decided by fourth-order terms in the oxygen-ion potential and correlation functions, together with strain interactions.

While the parameter values place LaAlO₃ within the trigonal phase, both theories show that SrTiO₃ is a borderline case slightly favoring the tetragonal structure.^{8,9} Indeed, studies by Burke and Pressley¹⁰ of Cr³⁺-impurity fluorescence-line splittings under uniaxial stress showed that 24.7 kg/mm² (1 kg/mm² = 98 bar) applied along a [111]-pseudocubic axis at 4.2°K, suffices to induce the trigonal phase.

The electron paramagnetic resonance (EPR) technique^{2,11} used in this work has the advantage of providing direct measures of components of

the order parameter $\bar{\varphi}$, obviating the crystal-field parameter fitting required to analyze effects of stress on Cr³⁺ fluorescence.¹² Another advantage of EPR is that accurate measurements are possible at higher temperatures, close to T_a , where Cr³⁺ fluorescence lines become broad.

In the experiments a stress p was applied along the axes of cylindrical samples parallel to a cubic [111] direction. The sample diameter was typically 1 mm, its height about 3 mm. Special care was necessary to polish parallel end planes and use Teflon sheets there to ensure homogeneous strain in the sample and reduce hysteresis effects at the first-order transitions. The nominal Fe₂O₃ content was 0.03%. The variable-temperature cryostat allowed the application of stress only perpendicular to the external magnetic field H . Under this geometry ($p \parallel [111]$) the EPR spectrum of Fe³⁺ substitutional for Ti⁴⁺ is insensitive to the octahedral rotation $\bar{\varphi}$ in the trigonal phase. However, the spectrum of the lower symmetry Fe³⁺-V_O pair center,¹³ i.e., a Fe³⁺ with a nearest-neighbor oxygen vacancy, does vary with φ_{111} . It has been used throughout this work taking into account the smaller rotation of this center, $\bar{\varphi}(\text{Fe}^{3+}-V_O) = \varphi/(1.59 \pm 0.05)$. This newly determined coefficient differs from the value 1.4 deduced earlier from Ref. 11.

Figure 1(a) shows the variation of a group of EPR lines with [111] stress for H parallel to a $[\bar{1}\bar{1}0]$ -pseudocubic direction at 78°K. It corresponds to but one line for $T > T_a$ and $p = 0$, which results from Fe³⁺-V_O pairs with symmetry axis at 45° to H , i.e., parallel to [100] and [010].¹³

For zero stress there are four lines. The outer two are both due to pairs located in [001] domains. These pairs lie on two inequivalent

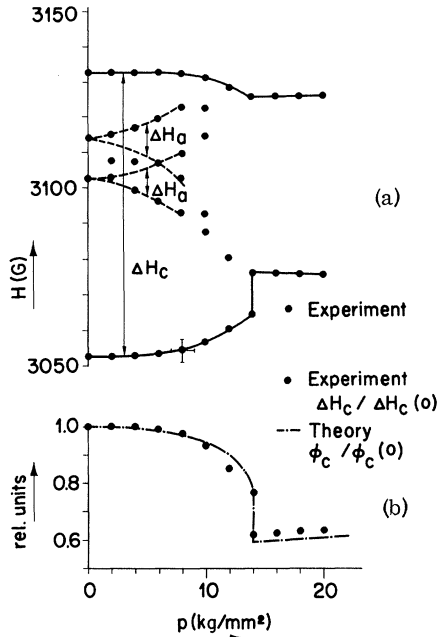


FIG. 1. (a) Splitting of EPR lines due to $\text{Fe}^{3+}-V_{\text{O}}$ centers for stress p parallel to a $[111]$ axis and $H \parallel [1\bar{1}0]$ at 78°K and 19.5 GHz . (b) Comparison of the splitting with the calculated tetragonal component of the rotation angle under $[111]$ stress. ($1\text{ kg/mm}^2 = 98\text{ bar}$).

octahedral sublattices rotated in both directions around the c axis ($c \parallel [001]$) and away from the a axes by an amount $\bar{\varphi} = (0.95 \pm 0.05)^\circ$, their splitting ΔH_c being proportional to φ_c . The two middle lines result from pairs in $[100]$ and $[010]$ domains. Their g tensors are either axial, if the pair axis is along a domain axis, or orthorhombic if these axes are perpendicular to one another. The (001) plane is a mirror plane for $\pm\bar{\varphi}$ rotations along the in-plane $[100]$ or $[010]$ domain axes yielding degenerate lines.¹⁴ Under $[111]$ stress the pair centers in the two sublattices of these domains become inequivalent, turning toward and away from H by proportionate amounts causing a splitting ΔH_a . For our particular geometry, ΔH_a is proportional to the components φ_{001} of $\bar{\varphi}$. Thus for $p > 0$ the spectrum arising from domains with three orientations of the pseudotetragonal c axis generally consists of three doublets split by ΔH_c and ΔH_a as seen in Fig. 1(a).

When p increases from zero, ΔH_c decreases and ΔH_a increases because $\bar{\varphi}$ is tilted away from the respective c axis toward $[111]$ in each domain. However, in this range of p , only the highest and lowest lines, whose difference gives ΔH_c , are sufficiently resolved for quantitative

discussion. Since the observed changes in H are small [$<2\%$ of $|H_{\parallel} - H_{\perp}|$] at all temperatures, ΔH_c is to good approximation linear in φ_{001} and independent of the rhombic shift. Of special interest is the behavior of the lowest line which at a critical stress $p_c(78^\circ\text{K}) = 14 \pm 1\text{ kg/mm}^2$ changes discontinuously. At p_c the lowest lines observed above and below this critical pressure coexist. We regard this as clear evidence for a first-order transition. Above p_c the spectrum coalesces into a pair of slowly varying degenerate lines resulting from $\pm\bar{\varphi}$ rotations around the $[111]$ direction parallel to the stress. Thus above p_c we have a monodomain SrTiO_3 sample with $R\bar{3}c$ structure.

The variation of $\bar{\varphi}$ with p has been calculated in a forthcoming paper on the stress dependence of Cr^{3+} fluorescence at 4.2°K .¹² The theory is based on a Landau configurational potential of the form^{12, 15}

$$\begin{aligned} \bar{U} = & \frac{1}{2}KQ^2 + A'Q^4 + A_n' \sum_{i < j} Q_i^2 Q_j^2 \\ & - b_e \sum_i T_{ii}(3Q_i^2 - Q^2) - b_t \sum_{i < j} T_{ij} Q_i Q_j. \end{aligned} \quad (1)$$

Here $Q_i (= \frac{1}{2}a\omega_i)$, where a is the lattice parameter) is a pseudocubic axial component of the soft-optic mode which lies at the $[111]$ corner of the Brillouin zone; T_{ij} is the applied stress tensor; $K(T)$ is a temperature-dependent parameter satisfying the condition $K(T_a) = 0$. At other $T < T_a$, $K(T)$ is taken proportional to $\varphi^2(T)$ measured at zero stress.² Values of the proportionality constant and the constants A' , A_n' , b_e , b_t have been established¹⁶ from experiments whose errors range up to $\pm 25\%$.

For the present case of $[111]$ stress ($T_{ij} = -\frac{1}{3}p$, all i, j), electronically computed results for $\bar{Q}(p)$ were given only for $T = 4.2^\circ\text{K}$.¹² The results may be scaled to other $T < T_a$ according to the law $\varphi^2 \propto Q_i^2 \propto K \propto p$, since this changes all terms in Eq. (1) only by a common factor. The normalized results for φ_c versus p at $T = 78^\circ\text{K}$ are compared with the experimental ΔH_c in Fig. 1(b). Rotating \bar{H} in the plane normal to stress in the trigonal phase at p slightly above p_c allowed the determination of $\bar{\varphi}_{\text{tr}}$ from the periodicity of the EPR spectrum. From this result, $\bar{\varphi}_{\text{tr}} = 1.06 \pm 0.10^\circ$, we obtain $\varphi_{\text{tr}}(p_c)/\varphi_{\text{tet}}(0) = \bar{\varphi}_{\text{tr}}/\bar{\varphi}_{\text{tet}} = 1.11 \pm 0.10$, which agrees with the calculated value 1.03.

Above T_a the $R\bar{3}c$ phase could also be induced with $[111]$ stress, as shown in Fig. 2(a) for $T - T_a = 1.0 \pm 0.5^\circ\text{K}$. The experimental setup was the same as for $T = 78^\circ\text{K}$ [Fig. 1(a)]. Due to the

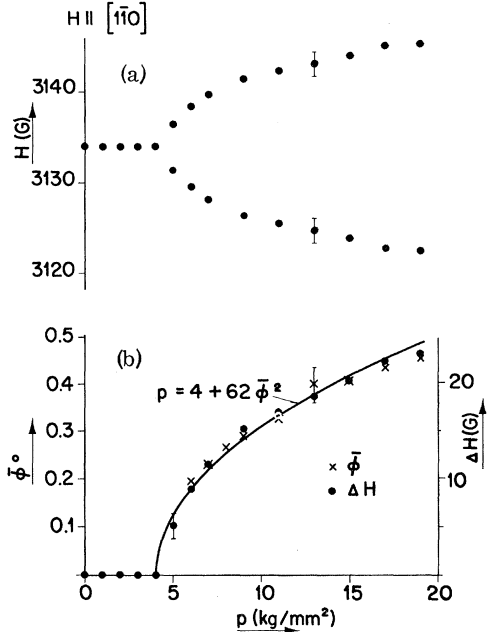


FIG. 2. (a) Splitting of EPR lines resulting from Fe³⁺-V_O centers for $p \parallel [111]$ and $H \parallel [1\bar{1}0]$ at 104°K. (b) Stress dependence of the splitting and rotation angle.

O_h^1 symmetry of the crystal at $p=0$ the four lines have collapsed into one. As p increases from zero the line remains unsplit up to a critical pressure p_c (104°K) = 4.0 ± 0.7 kg/mm² above which a parabolic splitting into two lines is observed. They result again from $\pm\bar{\varphi}_{ir}$ rotations due to an $R\bar{3}c$ monodomain crystal; the continuous splitting shows that the transition is of second order. Results for ΔH , and also for $\bar{\varphi}$ determined as before by rotating \vec{H} , are shown in Fig. 2(b). ΔH and $\bar{\varphi}$ are proportional to each other with a proportionality constant of 51 G deg⁻¹, which is identical to the value found at 78°K, thus proving the experimental consistency of our results.

Figure 3 shows experimentally determined critical stresses p_c and p'_c necessary to induce the $R\bar{3}c$ phase below and above T_a .¹⁷ Our value of p_c (4.2°K) agrees with one determined from Cr³⁺ fluorescence,¹⁰ which is also shown. As indicated above, the theoretical function $p_c(T)$ for $T < T_a$ is scaled from the one calculated point by direct proportion to published orthorhombic EPR splittings determined at zero stress,² which are proportional to φ^2 .⁸ We note in passing that at zero stress $\varphi(T)$ agrees within 5% with values calculated from the microscopic Hamiltonian containing only temperature-independent constants.⁹

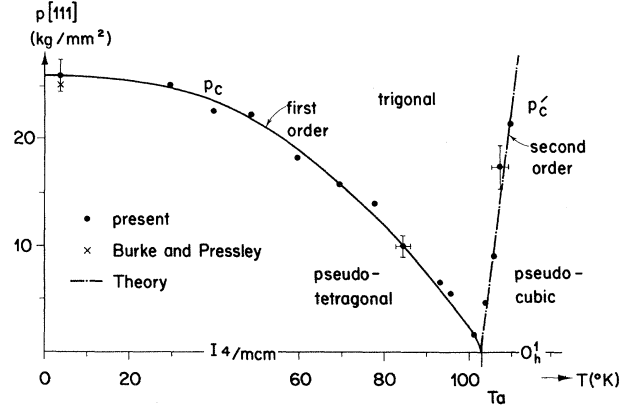


FIG. 3. Phase diagram of SrTiO₃ for stress-induced $R\bar{3}c$ phase. For $T < T_a$ the transition is first order, for $T > T_a$ second order.

In the case $T > T_a$ we have $K(T) > 0$, and \vec{U} as given in Eq. (1) is minimized analytically for $[111]$ stress with the result

$$(p - p'_c)\bar{\varphi}^{-2} = -\frac{1}{2}a^2(3A' + A_n')/b_t, \quad (2)$$

$$p'_c = -\frac{3}{2}K/b_t, \quad (3)$$

which holds for $p > p'_c$ and $b_t < 0$. In the case $p < p'_c$ we have $\vec{\varphi} = 0$.

The coefficient K is related to the soft-mode frequency ν according to

$$K(T) = 4\pi^2 M \nu^2(T), \quad T > T_a, \quad (4)$$

where M ($=0.897$ g cm⁻³) is the mass of two oxygen atoms per formula unit. Neutron inelastic scattering results at two laboratories^{5, 18} are consistent, for small $T - T_a > 0$, with the formula¹⁸ $\nu^2(T - T_a)^{-1} = (1.1 \pm 0.3) \times 10^{22}$ Hz²/K. Combining this result with Eqs. (3) and (4), using our parameter values,¹⁶ we find

$$p'_c = 3.1(T - T_a) \text{ kg/mm}^2, \quad T > T_a. \quad (5)$$

Thus, we obtain the two segments of the theoretical phase boundary shown in Fig. 3, in substantial agreement with the experimental points.

Figure 3 represents an unusual case of a well-understood diagram of uniaxial-stress-induced phase changes of a crystalline solid in a large temperature interval. Recent studies of soft-mode Raman scattering by Burke, Pressley, and Slonczewski¹⁹ as well as other effects mentioned^{8, 12} are accounted for by the same Landau potential.

For $p \geq p'_c$ (104°K) the data in Fig. 2(b) obey approximately the parabolic curve

$$(p - p'_c)\bar{\varphi}^{-2} = 62 \pm 11 \text{ kg mm}^{-2} \text{ deg}^{-2} \quad (6)$$

shown in the figure. Using the relation $\varphi/\bar{\varphi} = 1.59 \pm 0.05$ determined for $T < T_a$, Eq. (2) gives us, at all T ,

$$(p - p_c')\bar{\varphi}^{-2} = 162 \text{ kg mm}^{-2} \text{ deg}^{-2}. \quad (7)$$

In view of the good fit for $\bar{\varphi}$ versus $p(111)$ for $T = 78^\circ\text{K}$, and the temperature dependence of p_c and p_c' , the magnitude of the discrepancy between (6) and (7) is remarkably large. It may arise simply from errors in the parameter values, which combine differently below and above T_a to determine $\bar{\varphi}(p)$. A more interesting possibility is that critical-point fluctuations may cause departures from the thermodynamic theory when T differs from T_a by as little as 1%.

We acknowledge very fruitful discussions with Dr. J. Feder and Dr. E. Pytte on the results of the microscopic model Hamiltonian theory.

*Permanent address: IBM Thomas J. Watson Research Center, Yorktown Heights, N. Y. 10598

¹W. Cochran and A. Zia, Phys. Status Solidi 25, 273 (1968).

²K. A. Müller, W. Berlinger, and F. Waldner, Phys. Rev. Lett. 21, 814 (1968), and references quoted therein.

³H. Thomas and K. A. Müller, Phys. Rev. Lett. 21, 1256 (1968).

⁴P. A. Fleury, J. F. Scott, and J. M. Worlock, Phys. Rev. Lett. 21, 16 (1968).

⁵G. Shirane and Y. Yamada, Phys. Rev. 177, 858 (1969).

⁶J. D. Axe, G. Shirane, and K. A. Müller, Phys. Rev. 183, 820 (1969).

⁷J. F. Scott, Phys. Rev. 183, 823 (1969).

⁸J. C. Slonczewski and H. Thomas, Phys. Rev. B 1, 3599 (1970).

⁹E. Pytte and J. Feder, Phys. Rev. 187, 1077 (1969); J. Feder and E. Pytte, Phys. Rev. B 1, 4803 (1970).

¹⁰W. J. Burke and R. J. Pressley, Solid State Commun. 7, 1187 (1969).

¹¹H. Unoki and T. Sakudo, J. Phys. Soc. Jap. 23, 546 (1967).

¹²J. C. Slonczewski, Phys. Rev. (to be published).

¹³E. S. Kirkpatrick, K. A. Müller, and R. S. Rubins, Phys. Rev. 135, A86 (1964).

¹⁴An analysis of a center analogous to $\text{Fe}^{3+}\text{-}V_{\text{O}}$ in SrTiO_3 , the $\text{Ni}^{3+}\text{-}V_{\text{O}}$ center, has been described: K. A. Müller, W. Berlinger, and R. S. Rubins, Phys. Rev. 186, 361 (1969), although the orthorhombic g shifts for the $\text{Ni}^{3+}\text{-}V_{\text{O}}$ are so small that the two inner lines are not resolved.

¹⁵A similar potential was used by W. Rehwald, Solid State Commun. 8, 607 (1970).

¹⁶ $K(77^\circ\text{K}) = -1.59 \times 10^{25}$, $A' = 1.58 \times 10^{43}$, $A_n' = 6.19 \times 10^{42}$, $b_e = 7.34 \times 10^{14}$, $b_t = -1.98 \times 10^{15}$, all in cgs units. (b_e is B_e/C_e and b_t is B_t/C_t in previous notation; see Ref. 12.)

¹⁷The transition temperature $T_a = 103.0 \pm 1.0^\circ\text{K}$ appears to be lower than those published in the literature which range from 104°K to 108°K (Refs. 2, 4, and 5). It has been shown that T_a is depressed by 2°K per 0.1% oxygen vacancies (V_{O}) present [D. W. Deis, M. Ashkin, J. K. Hulm, and C. K. Jones, Bull. Amer. Phys. Soc. 15, 102 (1970)]. The Fe doping level in our sample, creating $\frac{1}{2}V_{\text{O}}$ per Fe^{3+} because of charge compensation, can depress T_a by no more than 1°K . Thus, the crystal used to fabricate the samples must have contained additional V_{O} 's, i.e., was insufficiently oxidized.

¹⁸R. A. Cowley, W. J. L. Buyers, and G. Dolling, Solid State Commun. 7, 181 (1969).

¹⁹W. J. Burke, R. J. Pressley, and J. C. Slonczewski, to be published.